MEASUREMENT IN BOUNDARY LAYER FLOWS – INDIVIDUAL REPORT

Name: Ioana Ispas

Student ID: 210061590

Module Code: EMS513U

Module Title: Aerothermodynamics of Flows

Coursework Name: Measurement in Boundary Layer Flows

Raw Data: Group 13

Apparatus and Instrumentation

The apparatus for this experiment consisted of an open circuit vertical wind tunnel with a smooth flat plate mounted in the working section parallel to the flow. A flattened pitot tube was attached at the mid-span position to allow pressure measurements to be taken from different traverse positions normal to the plate surface. This ensured that the surface pressure remained zero. The tube was connected to a manometer, where the pitot height could then be measured, and a tube from the airbox and one from the pitot tube were connected to an inclined water manometer, to use for collecting h_{box} and h_{pitot} values. A digital micrometre with a resolution of $1x10^{-3}$ was used to adjust the traverse mechanism. A mercury barometer and thermometer from the laboratory were used to measure the atmospheric pressure and temperature respectively.

Table 1: Raw data acquired from Manometer Readings

Raw Data for x = 0.115m				Raw Data for x = 0.265m			
Ym Micrometer Reading (mm)	hbox (mm)	hpitot (mm)	hopen (mm)	Ym Micrometer Reading (mm)	hbox (mm)	hpitot (mm)	hopen (mm)
0	220	182	144	0	220	178	144
0.2	220	204	144	0.2	220	188	144
0.4	220	210	144	0.4	220	190	144
0.6	220	212	144	0.6	220	194	144
0.8	220	216	144	0.8	220	198	144
1	220	216	144	1	220	198	144
1.2	220	216	144	1.2	220	200	144
1.4	220	218	144	1.4	220	202	144
1.9	220	218	144	1.9	220	208	144
2.4	220	218	144	2.4	220	210	144
2.9	220	218	144	2.9	220	214	144
3.4	220	218	144	3.4	220	216	144
3.9	220	218	144	3.9	220	218	144
4.4	220	218	144	4.4	220	218	144
4.9	220	218	144	4.9	220	218	144
5.4	220	218	144	5.4	220	218	144
5.9	220	218	144	5.9	220	220	144
6.4	220	218	144	6.4	220	220	144

Table 2: Raw Background data

Sutherland Constant/S (K)	Atmospheric Temperature (^oC)	Atmospheric Pressure (mmHg)	Thickness of pitot tube/d (mm)	Manometer angle/β (^{o})
111	19	739	1.02	60

Specific Gas Constant/$R_{specific}$ (J.Kg^-1.K^-1)	Density of water/ρ_{water} (Kg/m^3)	Gravitational Acceleration/g (m/s^2)	Reference Temperature/T_{ref} (K)	Reference viscosity/μ_{ref} (Ns/m^2)
287.058	1000	9.81	273	$1.7160*10^{-5}$

Sample Calculations

1. Density of Air:

$$\rho_{air} = \frac{p_{abs}}{R_{specific}T} = \frac{99.165 * 10^3}{287.058 * 292.15} = 1.18245\ kgm^{-3}$$

2. Viscosity of Air:

$$\mu_{air} = \left(\frac{T_{atm}}{T_{ref}}\right)^{1.5} * \left(\frac{T_{ref}+S}{T_{atm}+S}\right)\mu_{ref} = \left(\frac{19+273.15}{273}\right)^{1.5} * \frac{273+111}{19+273.15+111} * 1.716 * 10^{-5} = 1.80945 * 10^{-5} Nsm^{-2}$$

3. Delta h at Y_m= 0.2mm for x = 0.265m:

$$\Delta H = h_{pitot} - h_{open} = 188 - 144 = 44\ mmH2O$$

4. Value of y at 0.2mm for x = 0.265m:

$$y = Y_m + \frac{d}{2} = 0.2 + \frac{1.02}{2} = 0.71mm$$

5. Value of Dynamic head at 0.2mm for x = 0.265m:

$$Dynamic\ Head = \rho_{water} g \frac{\Delta h}{1000} Sin\beta = 1000 * 9.81 * \left(\frac{178-144}{1000}\right) * Sin(60) = 288.854\ Pa$$

6. Local Flow velocity at y= 0.510 for x = 0.265m:

$$U = \sqrt{\frac{2P_{DH}}{\rho_{air}}} = \sqrt{\frac{2 * 288.854}{1.18245}} = 22.10357 ms^{-1}$$

7. Reynolds number for x = 0.265m:

$$Re_{0.265} = \frac{\rho_{air} x U_\infty}{\mu_{air}} = \frac{1.18245*0.265*33.0468}{1.80945*10^{-5}} = 572285.38$$

8. Wall Shear Stress for x = 0.265m:

$$\tau_w = \mu_{air} * \frac{U_1}{y_1} = 1.80945 * 10^{-5} * \frac{22.10357}{0.51 * 10^{-3}} = 0.78422\ Pa$$

9. Skin Friction coefficient for x = 0.265m:

$$C_f = \frac{\tau_w}{0.5\rho U_\delta^2} = \frac{0.78422}{0.5 * 1.18245 * 33.046825^2} = 0.0012146$$

10. Boundary Layer Displacement Thickness as a Ratio of Boundary Layer Physical Thickness for x = 0.265m:

$$\frac{\delta^*}{\delta} = \int_0^1 (1 - \frac{U}{U_\delta})\, d\eta, where\ d\eta = \frac{y}{\delta}, = 0.13082007$$

11. Boundary Layer Momentum Thickness as a Ratio of Boundary Layer Physical Thickness for x = 0.265m:

$$\frac{\theta}{\delta} = \int_0^1 \frac{U}{U_\delta}(1 - \frac{U}{U_\delta})\, d\eta, where\ d\eta = \frac{y}{\delta}, = 0.07120519$$

12. Boundary Layer Displacement Thickness as a Ratio of Boundary Layer Physical Thickness for Blasius Solution (Gerhart, P.M. *et al.* (2016)):

$$\frac{\delta^*}{\delta} = \frac{\left(\frac{1.71811x}{\sqrt{Re_x}}\right)}{\left(\frac{5.2x}{\sqrt{Re_x}}\right)} = \frac{1.71811}{5.2} = 0.330405769$$

13. Boundary Layer Momentum Thickness as a Ratio of Boundary Layer Physical Thickness for Blasius Solution (Gerhart, P.M. *et al.* (2016)):

$$\frac{\theta}{\delta} = \frac{(\frac{0.664x}{\sqrt{Re_x}})}{(\frac{5.2x}{\sqrt{Re_x}})} = \frac{0.664}{5.2} = 0.12769$$

14. Wall shear stress for Blasius Solution (Gerhart, P.M. *et al.* (2016)):

$$\tau_w = \mu\left(\frac{\delta u}{\delta y}\right) = \frac{0.33206\rho U_\infty^2}{\sqrt{Re_x}} = \frac{0.33206 * 1.18245 * 32.6091^2}{\sqrt{2.45 * 10^5}} = 0.84341\ Pa$$

15. Theoretical Skin friction solution:

$$C_f = \frac{\tau_w}{0.5\rho U_\delta^2} = \frac{0.0577}{Re_x^{0.2}} = \frac{0.0577}{(5.72 * 10^5)^{0.2}} = 0.00407055$$

16. Boundary Layer Displacement Thickness as a Ratio of Boundary Layer Physical Thickness for Power Law (Gerhart, P.M. *et al.* (2016)):

$$\frac{\delta^*}{\delta} = \int_0^1 \left(1 - \eta^{\frac{1}{7}}\right) d\eta, where\ \eta = \frac{y}{\delta}, = \frac{1}{8}$$

17. Boundary Layer Momentum Thickness as a Ratio of Boundary Layer Physical Thickness for Power Law (Gerhart, P.M. *et al.* (2016)):

$$\frac{\theta}{\delta} = \int_0^1 \eta^{\frac{1}{7}}\left(1-\eta^{\frac{1}{7}}\right)d\eta \text{ , where } \eta = \frac{y}{\delta}, = \frac{7}{72}$$

(Same equation was used for finding the theoretical wall shear stress)

Table 3: Processed results for the experimental values

Processed data for x = 0.115m					Processed data for x = 0.265m				
y = Ym + d/2 (mm)	Dynamic Head (Pa)	U/ms-1	U/Uδ	y/δ	y = Ym + d/2 (mm)	Dynamic Head (Pa)	U/ms-1	U/Uδ	y/δ
-	-	-	0.000	0.000	-	-	-	0.000	0.000
0.510	322.837	23.368	0.717	0.298	0.510	288.854	22.104	0.669	0.0863
0.710	509.743	29.363	0.900	0.415	0.710	373.811	25.145	0.761	0.120
0.910	560.717	30.796	0.944	0.532	0.910	390.803	25.710	0.778	0.154
1.110	577.708	31.259	0.959	0.649	1.110	424.785	26.805	0.811	0.188
1.310	611.691	32.165	0.986	0.766	1.310	458.768	27.856	0.843	0.222
1.510	611.691	32.165	0.986	0.883	1.510	458.768	27.856	0.843	0.255
1.710	611.691	32.165	0.986	1.000	1.710	475.760	28.367	0.858	0.289
1.910	628.682	32.609	1.000	1.117	1.910	492.751	28.869	0.874	0.323
2.410	628.682	32.609	1.000	1.409	2.410	543.725	30.326	0.918	0.408
2.910	628.682	32.609	1.000	1.702	2.910	560.717	30.796	0.932	0.492
3.410	628.682	32.609	1.000	1.994	3.410	594.700	31.716	0.960	0.577
3.910	628.682	32.609	1.000	2.287	3.910	611.691	32.165	0.973	0.662
4.410	628.682	32.609	1.000	2.579	4.410	628.682	32.609	0.987	0.746
4.910	628.682	32.609	1.000	2.871	4.910	628.682	32.609	0.987	0.831
5.410	628.682	32.609	1.000	3.164	5.410	628.682	32.609	0.987	0.915
5.910	628.682	32.609	1.000	3.456	5.910	628.682	32.609	0.987	1.000
6.410	628.682	32.609	1.000	3.749	6.410	645.674	33.047	1.000	1.085
6.910	628.682	32.609	1.000	4.041	6.910	645.674	33.047	1.000	1.169

Table 4: Results for Experimental and Theoretical data

	x (m)	Re	δ/x	δ*/δ	θ/δ	H	τ_w (Pa)	C_f
Experimental Results at x =0.115	0.115	2.45*10^5	0.0149±0.00004	0.235±0.00006	0.0674±0.002	3.50±0.150	0.829±0.030	0.00132±0.00013
Experimental Results at x =0.265	0.265	5.72*10^5	0.0223±0.00004	0.131±0.00006	0.0712±0.003	1.84±0.170	0.784±0.060	0.00121±0.00016
Blasius Solution	0.115	2.45*10^5	0.0105±0.00003	0.33±0.00002	0.128±0.000011	2.588±0.004	0.843±0.003	0.00134±0.00009
Power Law (Turbulent) Solution	0.265	5.72*10^5	0.0261±0.00008	0.125±0.00007	0.0972±0.000014	1.286±0.006	2.628±0.009	0.00407±0.00010

Table 5: Processed data for calculations

Viscosity of Air/μair (Pa.s)	Density of Air/ρ_{air} (kg/m^3)	Absolute Pressure/p_{abs} (Pa)	Absolute Temperature/T_{abs} (K)
1.80945*10-5	1.182	98525.2	292.15

Results

Figure 1: Graph showing the velocity profiles for experimental and theoretical data against the distance from the surface of a flat plate

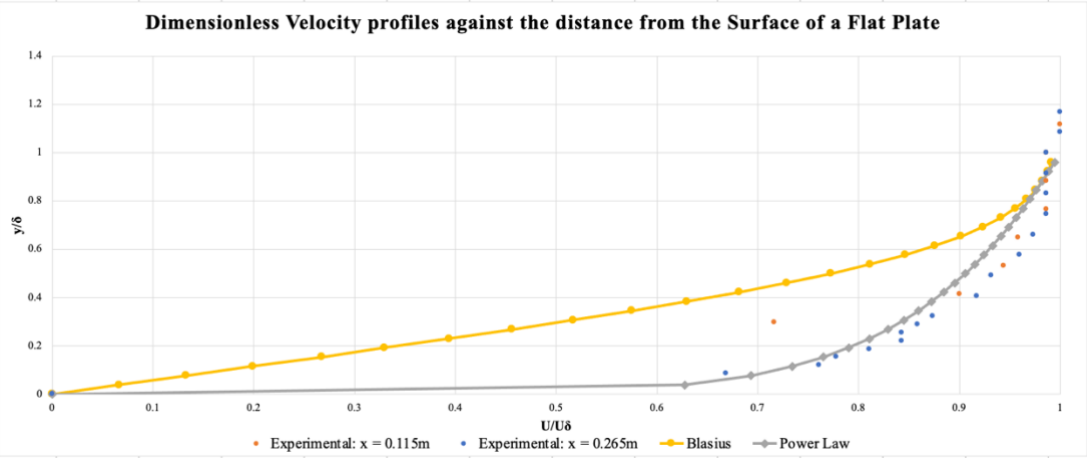

Discussion

Learning outcome:

The learning outcomes of this experiment included identifying and understanding the changes in the velocity profile of boundary layer flows at different traverses on a flat plate based off changes in Reynolds number as the distance from the leading edge is increased, and comparing the results procured to theoretical representations of turbulent and laminar flows (Power Law and Blasius solutions).

Perceived difficulties encountered:

The water levels would fluctuate constantly, making it difficult to produce an accurate result. Parallax errors due to the fluctuation of the water bubbles were also a cause of inaccurate results. We allowed 30 seconds between readings to ensure the fluctuation stopped before taking the measurements. The micrometre was also extremely sensitive, which proved to be a difficulty when increasing the reading as it would take a few tries to get the right y value for the measurements.

General trends:

As the airflow moves further away from the leading edge, the Reynolds number increases, meaning that the flow becomes more turbulent. This is seen in the experimental values in Table 4, where the Reynolds number is significantly higher at x=0.265 m. As seen in Figure 1, the experimental values are transitional. This experiment looks at one boundary layer, so the shape of the velocity profiles at the leading edge onwards determines a laminar trend as seen in the Blasius plot line, and then starts assuming a steeper velocity gradient at a further distance of x, as generally seen in turbulent flows. This is expected, as both Reynolds numbers are in the critical value order of $Re_{xcr}=2x10^5$ to $3x10^6$. [Gerhart P.M et al., 2016]. It is further evident that both x values produce turbulent boundary layers due to the steep velocity gradient at the wall and the discrepancy of the results close to its free stream velocity, as seen in Figure 1. The further the particles travel downstream, the more turbulent the particles become, thus increasing the number of disturbances.

Furthermore, when considering airflow on a flat plate, the further the airflow moves from the leading edge, the thicker the boundary layer becomes due to the assumption that there is no pressure gradient. This leads to higher free stream velocity values for x values further from the leading edge, and a steeper velocity gradient on the graph. When observing the results for the experimental values, it is evident that the results correlate with the theories, due to the increase in boundary layer thickness at 0.265 m. An increase in boundary layer thickness leads to a decrease in wall shear stress, for which the contrast between experimental values is displayed in Table 4. This also leads to a decrease in the shape factor. The higher the value of the shape factor, the more likely it is for boundary layer separation to occur. As shown in Table 4, the shape factor is higher for x at 0.115 m, as it has a lower Reynolds number and is therefore closer in resemblance to laminar flow, meaning it has a thinner boundary layer and thus more chances of boundary layer separation taking place than at 0.215 m.

Possible Improvements:

Table 6: Error percentages

	δ/ x (%)	δ*/δ (%)	θ/δ (%)	H (%)	τ_W (%)	C_f(%)
Experiment	0.2685	0.0255	2.9674	4.2860	3.6184	10.0000
Experiment	0.1794	0.0459	4.2135	9.2532	7.6511	13.3333
Blasius	0.2857	0.0061	0.0086	0.1546	0.3558	0.6923
Power Law	0.3065	0.0560	0.0144	0.4667	0.0030	2.4390

Based off the difficulties experienced, reducing parallax error by repeating the experiment three times for each value procured and concluding an average would allow for more accurate measurements. Leaving more time in-between readings is also necessary, to ensure that the readings cease to fluctuate. A time of 60 seconds in-between each reading should ensure the best results. Another improvement regarding the experiment would be to take measurements at more values of x. This would provide more experimental data to compare the behaviour of the flow more accurately for different distances from the leading edge.

Conclusion

Overall, this experiment has shown that as the air flows further from the leading edge, its Reynolds number increases, and it begins to transition from a laminar to a turbulent flow when $Re_x > Re_{xcr}$. This proves that the Reynolds number is an important factor when viewing boundary layer flows, as it can determine the type of flow and relative thickness of the boundary at different points on a flat plate. The uncertainty values for this experiment were small, ensuring that the data was reliable, and the experiment values matched the trend of the theoretical data as shown in Figure 1, thus concluding that this experiment was a success.

References

Anderson, J.D. and Bowden, M.L. (2016) *Introduction to flight*. New York, NY: McGraw-Hill. (Pages 236-250)

Frank M. White (1) (2011) Fluid Mechanics 7th Edition, McGraw Hill, Chapters: 7.3-7.4

Gerhart, P.M. *et al.* (2016) *Munson, young and Okishi's fundamentals of Fluid Mechanics*. Hoboken, NJ: John Wiley & Sons, Inc. (Pages 418-429)

Hermann Schlichting & Klaus Gersten, Boundary Layer Theory Ninth Edition (2017), Springer, Chapters; 2.2 & 2.3 (Pages 30 – 36)